ELSEVIER

Agricultural and Forest Meteorology 85 (1997) 87–98

AGRICULTURAL AND FOREST METEOROLOGY

An improved method for estimating surface humidity from daily minimum temperature

J.S. Kimball *, S.W. Running, R. Nemani

NTSG School of Forestry, University of Montana, Missoula, MT 59812, USA

Accepted 19 June 1996

Abstract

Minimum daily air temperature (T_n) is often used as a surrogate for mean daily dew point ($T_{d,day}$) to estimate near-surface humidity. This method is unreliable under arid conditions where nightly minimum temperatures may remain well above the dew point. Daily meteorological data from 52 weather stations within the continental US and Alaska were evaluated. Daily differences between $T_{d,day}$ and T_n were large in arid climates, with corresponding vapor pressure differences averaging between 0.8 and 1.2 kPa on an annual basis. Sites with semi-arid characteristics showed a large degree of seasonality in the results with average vapor pressure differences ranging from 0.1 to 0.6 kPa between winter and summer months. Sites in other climate regimes generally showed small differences between T_n and $T_{d,day}$ over the entire year, corresponding to average vapor pressure differences of less than 0.3 kPa. An empirical model was developed to improve the accuracy of T_n based humidity estimates using daily air temperature, annual precipitation and estimated daily potential evapotranspiration. The model reduced humidity estimation errors by up to 80% at semi-arid and arid sites and had minimal effects when T_n based humidity estimates were relatively accurate. The ratio of annual precipitation to estimated annual evapotranspiration was useful for distinguishing sites where T_n based humidity estimates were relatively accurate from sites where estimation errors were large. The results of this investigation provide a simple, more accurate method than T_n for estimating humidity in arid and semi-arid regions using general weather station data. © 1997 Elsevier Science B.V.

1. Introduction

Humidity is an important parameter in ecological and hydrologic research because it strongly influences the transfer of moisture between the surface and atmosphere, and the water balance at local to regional scales. Low humidities increase the atmospheric demand for moisture and have been found to cause partial to full stomatal closure in plants, resulting in reduced transpiration, photosynthesis and plant productivity (Korner and Bannister, 1985; Choudhury and Monteith, 1986). Over longer temporal scales, humidities may influence plant evolutionary adaptations such as leaf area and cuticle thickness (Grantz, 1990). These factors influence soil moisture and runoff at local scales and may influence precipitation and atmospheric circulation patterns at regional to global scales (Hansen et al., 1984).

The Vegetation/Ecosystem Modeling and Analysis Project (VEMAP) and the Pottsdam Institute for Climate Change's Net Primary Productivity project (PIK-NPP) represent national and international efforts to (1) understand the interactions between climate, biosphere and biogeochemical processes at

* Corresponding author.

0168-1923/97/$17.00 © 1997 Elsevier Science B.V. All rights reserved.
PII S0168-1923(96)02366-0

regional to global scales and (2) assess the response of the biosphere to global climate change. These efforts have been hampered by a general lack of dependable, daily humidity data from the current global network of weather stations (Friend, 1996; Kittel et al., 1996). In the US, humidity is generally measured only at primary National Weather Service stations. Running et al. (1987) estimated this humidity measurement network to be less than 1 station per 100 000 km^2 throughout the western US. Primary weather stations are also predominantly located at lower elevations adjacent to airports, leaving higher elevations of the western US severely under-represented. Reliable, direct measurements of humidity generally require sensitive dew point hygrometer, chemical or electrical-type instruments. These sensors are prone to error and measurement accuracies may degrade over time without frequent sensor calibration (Marks et al., 1992; Glassy and Running, 1994). These problems underscore the need for efficient, indirect methods of estimating humidity over large regions in support of regional to global scale ecological modeling efforts.

Minimum daily air temperature (T_n) is a commonly measured parameter at weather stations and has been used in place of mean daily dew point ($T_{d,day}$) measurements to estimate humidity based on observations that (1) dew point and night minimum temperatures tend to come into equilibrium, and (2) the dew point remains relatively constant over the day (Running et al., 1987; Glassy and Running, 1994). Assumptions of T_n and $T_{d,day}$ equivalency are generally valid when condensation occurs during the night. This method is unreliable, however, under arid conditions where T_n may remain well above $T_{d,day}$, or under conditions where the dew point shows pronounced diurnal variation. The objectives of this investigation were to assess the relationships between T_n and $T_{d,day}$ under variable meteorological conditions, to develop a method for improving T_n based humidity estimates using general weather station data.

2. Theory

Humidity is a general term referring to the moisture content of the atmosphere. Two common measures of humidity are vapor pressure (e_a) and dew point (T_d); e_a refers to the component of atmospheric pressure exerted by water vapor. At constant air pressure and temperature, e_a varies only with changes in the water content of the atmosphere. T_d refers to the temperature at which the atmosphere becomes saturated. T_d remains constant unless water is added to or removed from the atmosphere. The gap between air temperature and T_d often decreases at night due to radiative cooling of the atmosphere near the surface. The air temperature may decrease until it reaches T_d and the air is at saturation. If the air temperature continues to decrease, water is removed from the atmosphere by condensation and both the air temperature and T_d remain approximately equal.

T_d has been found to stay relatively constant during the day (McCutchan, 1977; Finklin, 1983; Running et al., 1987; Glassy and Running, 1994). Observations have also shown that nightly minimum temperatures tend to come into equilibrium with T_d (James, 1953; Running et al., 1987). Because of these characteristics, T_n is often used as an indirect measure of $T_{d,day}$ owing to the generally greater accuracy and density of air temperature observations. The relationship between T_n and $T_{d,day}$, however, is strongly dependent on the climate characteristics of a particular region. Friend (1996) found that T_n provided good estimates of global scale humidities in Europe and North America but not in Africa. Running et al. (1987) also found that the correlation between T_n and $T_{d,day}$ deteriorated in arid environments.

The usefulness of T_n may be extended by incorporating additional information about climate characteristics. Air temperature and precipitation have traditionally been the most readily available data for describing and characterizing humidity and general climate characteristics. Köppen (1931) sought to classify world climates based on annual and monthly averages of temperature and precipitation, which were then related to major natural vegetation types. Thornthwaite (1948) used fractions of monthly and annual precipitation over potential evapotranspiration as a measure of regional humidity characteristics to define major humidity provinces. Friend (1996) demonstrated that precipitation in conjunction with minimum daily air temperature information significantly improved global scale humidity estimates.

3. Methods

Daily meteorological data were obtained from the National Climatic Data Center's TD-3210 Summary of the Day—First Order database (National Weather Service, 1988). These data are a synthesis of hourly data obtained under the National Weather Service's (NWS) Cooperative Program Automated Surface Observing System (ASOS). The data include daily mean, maximum and minimum air temperatures, mean daily dew point and daily precipitation from approximately 1987 through 1994. Data from 52 stations within the continental US and Alaska were selected for this investigation. Study sites were selected on the basis of data completeness and diversity of meteorological conditions. Station data were segregated into a development group of 20 stations and a test group of 32 stations. Meteorological data from the development group were used for model development while both data groups were used for model testing and validation.

Mean daily net solar radiation was estimated at each of the study sites and used with daily meteorological data to estimate daily potential evapotranspiration ($l_{\mathrm{Ep,day}}$). The ratio of $l_{\mathrm{Ep,day}}$ to annual precipitation, $l_{\mathrm{P,ann}}$, was used as a daily index of evaporative demand at each station location. Multiple linear regression techniques were used to quantify relationships between daily air temperature, $T_{\mathrm{d,day}}$ and daily ratios of $l_{\mathrm{Ep,day}}$ to $l_{\mathrm{P,ann}}$ for the model development station data group. Regression results were then applied using daily meteorological data for all stations to estimate $T_{\mathrm{d,day}}$. Measured and estimated dew point data were then converted to vapor pressures following Weast (1983). The standard error of the estimate (SEE) provides a useful measure of the mean variability between two quantities (Hogg and Ledolter, 1987). Standard errors of the estimate were computed between measured and estimated humidities for each of the 52 stations and used with regression results to evaluate T_{n} based humidity estimates.

3.1. Potential evapotranspiration

Potential evapotranspiration (E_{p}) is the upward limit of the evapotranspiration rate over a sufficiently moist surface under prevailing meteorological conditions (Brutsaert, 1982). Under these conditions, E_{p} represents the evaporative demand of the atmosphere. For this investigation the ratio of estimated $l_{\mathrm{Ep,day}}$ to $l_{\mathrm{P,ann}}$, was used as an index of relative aridity for each station. Mean daily E_{p} was estimated following the formulation of Priestley and Taylor (1972)

$$E_{\mathrm{p}} = \{\alpha[\Delta/(\Delta+\gamma)](R_{\mathrm{n}} - G)\}/\lambda \qquad (1)$$

where E_{p} is potential evapotranspiration (kg m^2 s^{-1}), Δ is the rate of change of saturation vapor pressure with temperature (Pa K^{-1}), γ is the psychrometer constant (approximately 0.66 Pa K^{-1}), R_{n} is the average daily net all-wave radiant energy flux (W m^{-2}), G is the average daily surface conductive energy flux (W m^{-2}), λ is the latent heat of vaporization (J kg^{-1}), and α is the Priestley–Taylor parameter (dimensionless).

The ratio of $E_{\mathrm{p,day}}$ to $l_{\mathrm{P,ann}}$ was estimated as

$$EF = \left[(E_{\mathrm{p}}/\rho_{\mathrm{w}})t_{\mathrm{day}})\right]/l_{\mathrm{P,ann}} \qquad (2)$$

where $EF = l_{\mathrm{Ep,day}}/l_{\mathrm{P,ann}}$, ρ_{w} is the density of water (kg m^{-3}), t_{day} is daylength (s), and $l_{\mathrm{P,ann}}$ is annual precipitation (m). t_{day} was defined as the period when the sun was above the horizon and was estimated from station latitude information following Hungerford et al. (1989).

The Priestley–Taylor formulation in Eq. (1) is a simplification of the Penman–Monteith approach whereby bulk stomatal, soil and aerodynamic resistances to soil–plant–atmosphere water movement are represented by a dimensionless coefficient, α. Priestley and Taylor found that approximately 80% of the evaporation rate was controlled by available radiant energy ($R_{\mathrm{n}} - G$) while adiabatic energy accounted for 21–22% of evaporation (i.e. $\alpha \cong 1.26$) for extensive, saturated land and water surfaces. This observation has been substantiated by other investigators for a variety of surface cover types (Monteith and Unsworth, 1990).

The Priestley–Taylor method was used to provide an approximation of the daily evaporative demand at each study site. This method is relatively simple and does not account for additional contributions to the evaporative flux from energy supplied by advection. However, while other methods may provide more accurate estimates of E_{p}, most are more data intensive and are not readily supported by general weather station data. A high degree of accuracy in calculating

E_p was not possible since various assumptions and simplifications of model inputs were required due to the limited nature of the daily input data. To simplify calculation, α was assigned a constant value of 1.26 and G was estimated as 10% of R_n (Campbell, 1977); Δ, λ and ρ_w were estimated from mean daily air temperature information using methods described by Running and Coughlan (1988).

3.2. Net radiant energy

The net all-wave radiation (R_n) at a point is the incident spectral irradiance less spectral exitance integrated over all wavelengths. Solar radiation represents the range of the electromagnetic spectrum from 0.3 to 3.0 μm while thermal radiation exists over much longer wavelengths from 3.5 to 50 μm. Thermal radiation is an important component of R_n under forested canopies, while solar radiation is most important in open areas. Net thermal radiation can be estimated when surface temperatures are known; however, since surface temperature information is generally not available at atmospheric weather stations, the contribution of net thermal radiation to the net all-wave radiation was ignored and R_n was assumed approximately equal to net solar radiation.

The net solar radiation at a point can be defined as

$$R_{n,s} = R_s(1.0 - \rho) \tag{3}$$

where $R_{n,s}$, R_s and ρ are the mean daily net solar radiation (W m^{-2}), solar irradiance (W m^{-2}) and solar albedo, respectively. Accurate measurements of solar irradiance and albedo require sensitive and costly instrumentation that is not readily available at most weather stations. For the purposes of this investigation ρ was assigned a constant value of 0.2. At each site, R_s was estimated over a flat surface at approximate 10 min intervals and integrated over t_{day} using the approach described by Hungerford et al. (1989). This approach calculates both direct and diffuse solar irradiance at the surface and adjusts for cloudcover effects using the difference between the daily maximum and minimum air temperatures (Bristow and Campbell, 1984). More detailed models of radiation transfer exist which can potentially achieve a high level of accuracy if surface albedo and atmospheric turbidity information is available. The approach described by Hungerford et al. was selected because it is relatively simple, robust and efficient. This method also requires minimal input data and can be readily applied at most weather stations.

4. Station climatological characteristics

A summary of site information including $l_{P,ann}$ and estimated annual potential evapotranspiration ($l_{Ep,ann}$) for the 52 stations in this investigation is presented in Table 1. Estimated annual potential evapotranspiration ranged from 2.0 m at arid sites to 0.7 m for sites in subpolar regions. The magnitude of $l_{Ep,ann}$ was mainly dependent on R_n which was regulated by station latitude and weather conditions. Arid stations were generally located in the southwestern US and were characterized by relatively long days with predominantly clear-sky conditions over most of the year. Stations in humid subtropical locations were located at similar latitudes but exhibited lower $l_{Ep,ann}$ due to greater numbers of cloudy days over the course of the year which reduced daily R_n. Stations in subpolar locations showed the lowest $l_{Ep,ann}$ owing to the reduced amount of solar radiation received over the year at higher latitudes.

Stations under arid and semi-arid conditions generally had the lowest annual precipitation, averaging 0.2 and 0.3 m, respectively. Annual precipitation was much more variable within other climate regions, ranging from 0.2 m in Fairbanks, AK to 1.9 m in Astoria, OR. Annual precipitation also averaged less than 20% of $l_{Ep,ann}$ at arid and semi-arid sites while $l_{P,ann}$ averaged greater than 66% of $l_{Ep,ann}$ in other regions.

Minimum daily air temperatures were relatively warm at arid, humid subtropical and coastal Mediterranean-marine sites, with respective annual averages of approximately 12, 11 and 9°C. Minimum daily air temperatures were cooler within other climate regimes, averaging from 4.9°C at semi-arid sites to 1°C at subpolar sites. Mean daily dew point temperatures tended to be greater within humid subtropical, coastal Mediterranean-marine and humid continental climate regimes, with respective annual averages of approximately 10, 7 and 3°C. Semi-arid, arid and subpolar sites were generally drier with $T_{d,day}$ annual

Table 1
Summary of weather station information

	Latitude (°N)	Longitude (°W)	Z (m)	Year	$l_{P,ann}$ (m)	$l_{Ep,ann}$ (m)	Major climatic region [a]
Development group							
China Lake, CA	35.41	117.41	681	1989	0.05	1.99	Arid
Las Vegas, NV	36.05	115.10	661	1991	0.11	1.94	Arid
Juneau, AK	58.22	134.35	7	1990	1.46	0.61	Subpolar
Salt Lake City, UT	40.47	111.58	1288	1994	0.40	1.65	Semi-arid
Spokane, WA	47.38	117.32	721	1994	0.38	1.30	Semi-arid
New Orleans, LA	29.57	90.00	2	1992	2.09	1.84	Humid–subtropical
Reno, NV	39.30	119.47	1341	1994	0.14	1.71	Semi-arid
Topeka, KS	39.04	95.37	270	1994	0.76	1.57	Humid continental
Springfield, IL	39.45	89.41	188	1987	0.74	1.53	Humid continental
San Diego, CA	32.44	117.10	11	1993	0.50	1.21	Coastal Mediterranean
Abiline, TX	32.26	99.41	535	1989	0.71	1.94	Semi-arid
Seattle, WA	47.27	122.18	137	1994	0.89	1.11	Coastal Mediterranean
Eugene, OR	44.07	123.13	114	1994	1.19	1.37	Coastal Mediterranean
Richmond, VA	37.30	77.20	50	1990	1.07	1.66	Humid subtropical
Madison, WI	43.08	89.20	266	1992	0.82	1.26	Humid continental
Charleston, SC	32.54	80.02	15	1987	1.42	1.79	Humid subtropical
Boston, MA	42.22	71.02	9	1991	1.07	1.22	Humid continental
Cleveland, OH	41.24	81.51	245	1988	0.76	1.36	Humid continental
Pierre, SD	44.23	100.17	531	1994	0.53	1.40	Humid continental
Tucson, AZ	32.07	110.56	779	1994	0.31	2.17	Arid
Test group							
Astoria, OR	46.09	123.53	7	1994	1.94	0.98	Marine
Boise, ID	43.36	116.12	825	1991	0.25	1.50	Semi-arid
Tulsa, OK	36.12	95.54	206	1994	1.27	1.67	Humid subtropical
Fargo, ND	46.54	96.48	273	1989	0.50	1.23	Humid continental
Lincoln, NE	40.51	96.45	360	1989	0.61	1.54	Humid continental
Casper, WY	42.55	106.28	1612	1994	0.36	1.57	Semi-arid
Little Rock, AR	34.44	92.13	79	1989	1.25	1.67	Humid subtropical
Billings, MT	45.48	108.32	1088	1994	0.36	1.42	Semi-arid
Pendleton, OR	45.41	118.51	456	1994	0.32	1.41	Semi-arid
Detroit, MI	42.15	83.19	202	1992	0.95	1.24	Humid continental
Albuquerque, NM	35.03	106.37	1620	1994	0.30	1.93	Semi-arid
Miami, FL	25.55	80.17	4	1992	1.47	1.76	Humid subtropical
Huntsville, AL	34.42	86.35	184	1993	1.32	1.73	Humid subtropical
Asheville, NC	35.26	82.29	639	1993	0.98	1.65	Humid subtropical
Des Moines, IA	41.31	93.38	295	1993	1.43	1.26	Humid continental
Portland, ME	43.39	70.19	190	1993	1.12	1.20	Humid continental
Fresno, CA	36.47	119.42	103	1991	0.28	1.81	Semi-arid
Winnemucca, NV	40.54	117.48	1311	1993	0.21	1.58	Semi-arid
Bishop, CA	37.22	118.22	1253	1993	0.16	1.85	Semi-arid
Phoenix, AZ	33.26	112.01	337	1994	0.23	2.10	Arid
Fairbanks, AK	64.49	147.52	138	1991	0.25	0.75	Subpolar
Harrisburg, PA	40.13	76.51	104	1990	1.14	1.43	Humid continental
Anchorage, AK	61.10	150.01	40	1994	0.34	0.67	Subpolar
Denver, CO	39.46	104.53	1626	1990	0.44	1.65	Semi-arid
South Bend, IN	41.45	86.10	244	1987	0.89	1.36	Humid continental
Grand Junction, CO	39.07	108.32	1477	1990	0.22	1.73	Semi-arid
Augusta, GA	33.22	81.58	41	1987	1.05	1.87	Humid subtropical
Diluth, MN	46.50	92.11	434	1988	0.83	1.17	Humid continental
Knoxville, TN	35.58	83.55	299	1988	0.89	1.72	Humid subtropical

Table 1 (continued)

	Latitude (°N)	Longitude (°W)	Z (m)	Year	$l_{P,ann}$ (m)	$l_{Ep,ann}$ (m)	Major climatic region [a]
Jackson, MS	32.19	90.05	89	1991	1.61	1.86	Humid subtropical
Louisville, KY	38.13	35.40	164	1988	0.96	1.60	Humid subtropical
Concord, NH	43.12	71.31	103	1991	1.01	1.35	Humid continental

[a] Köppen (1931).

averages of less than 2°C. All sites exhibited daily and seasonal variations in temperature trends ranging between seasonal maxima from April to October and minima from November to March. Coastal Mediterranean and marine sites showed the least variability, with standard deviations from mean annual dew point and minimum daily air temperatures of approximately 5°C. Temperatures were more variable within other climate regimes, with standard deviations from annual mean temperatures ranging from approximately 8°C at arid, semi-arid and humid subtropical sites to 10°C at subpolar and humid continental sites.

Annual plots of T_n and $T_{d,day}$ for three selected sites illustrate three major trends that were observed in the data (Fig. 1). Arid sites showed large daily differences between T_n and $T_{d,day}$ over the entire year, averaging 11°C. These results corresponded to mean daily differences between vapor pressures derived from $T_{d,day}$ ($e_{a,day}$) and T_n based vapor pressure estimates ($e_{a,Tn}$) from 0.8 to 1.2 kPa. The magnitudes of these differences were generally greatest between April and October during the warmest period of the year.

Differences between T_n and $T_{d,day}$ in semi-arid locations were generally smaller than differences at arid sites, averaging approximately 5°C over the entire year. Semi-arid sites generally showed close agreement between T_n and $T_{d,day}$ from November to March when daily air temperatures were cooler. Daily differences under these conditions averaged 2°C, corresponding to differences of approximately 0.1 kPa between $e_{a,Tn}$ and $e_{a,day}$. Daily differences were generally much greater between April and October, averaging 7.0°C and 0.6 kPa. Sites characterized by marine, coastal Mediterranean, humid continental, subpolar and humid subtropical conditions generally showed small differences between T_n and $T_{d,day}$ over the entire year, averaging less than 1.0°C. Average differences between $e_{a,day}$ and $e_{a,Tn}$ at these sites were less than 0.3 kPa.

The data also showed that $T_{d,day}$ was often greater than T_n. This pattern was observed at all sites, but less often at arid and semi-arid locations where

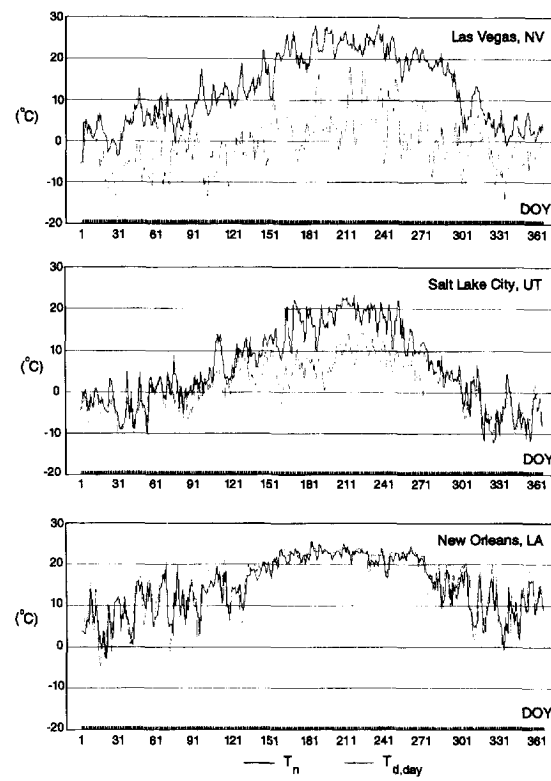

Fig. 1. Annual plots of mean daily dew point ($T_{d,day}$) and minimum daily air temperatures (T_n) for three selected sites. Plots illustrate three general characteristics of the database where: temperature differences are large over most of the year (Las Vegas, NV); temperature differences show a marked seasonal pattern ranging between winter minima and summer maxima (Salt Lake City, UT); temperature differences are minimal over the year (New Orleans, LA).

differences between $T_{d,day}$ and T_n were greater. Observations of $T_{d,day} > T_n$ in the data may reflect diurnal variations in the amount of water vapor in the air. T_n represented a single measurement made within a 24-h period while $T_{d,day}$ constituted an average of hourly measurements obtained over a 24-h period. It has generally been observed that T_d remains fairly constant during the day (Running et al., 1987; Glassy and Running, 1994). $T_{d,day}$ may be greater than T_n, however, if the amount of water vapor in the air increases during the day. Kaufmann (1984) confirmed this phenomenon by observing mid-day increases in absolute humidities for weather stations in Colorado. Kaufmann also found that ambient absolute humidities were consistently higher than nocturnal or early morning absolute humidities. Temperature differences when $T_{d,day}$ was greater than T_n were generally small, averaging approximately 2°C for the development and test group data. Instances where $e_{a,day}$ was greater than $e_{a,Tn}$ averaged approximately 0.11 kPa and were generally less than 0.22 kPa.

5. Model development and test results

Scatter plots showing a least-squares, linear fit of the relationship between $T_{d,day}$ and T_n, and the corresponding relationship between $e_{a,day}$ and $e_{a,Tn}$ for the development group data are presented in Fig. 2. T_n explained approximately 66% of the variation in $T_{d,day}$ with a standard error of 5.4°C. Corresponding values of $e_{a,Tn}$ explained 59% of the variation in $e_{a,day}$ with a standard error of 0.41 kPa. Regression results also indicated that $e_{a,Tn}$ was approximately 21% greater than $e_{a,day}$. Magnitudes of the differences between $e_{a,Tn}$ and $e_{a,day}$ were generally greater as T_n increased. This pattern reflected two general characteristics of the data. Warmer minimum daily air temperatures were more common in arid and semi-arid locations where differences between T_n and $T_{d,day}$ tended to be larger than other sites. The exponential nature of the relationship between temperature and humidity also resulted in much larger differences between $e_{a,day}$ and $e_{a,Tn}$ at warmer air temperatures given the same differences between $T_{d,day}$ and T_n (Weast, 1983). A 5°C difference between T_n and $T_{d,day}$ at an air temperature of approximately 3°C, for example, corresponded to a 0.2 kPa difference between $e_{a,Tn}$ and $e_{a,day}$. The same 5°C difference at 30°C resulted in an approximate 5-fold increase in the humidity estimation error to 1.0 kPa.

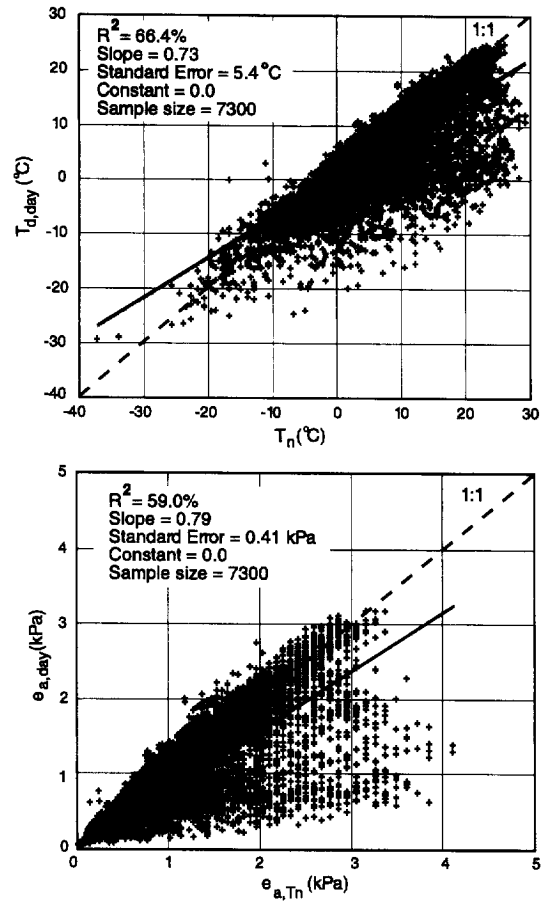

Fig. 2. Scatter plots showing the least-squares, linear regression results between $T_{d,day}$ and T_n, and the corresponding regression results between $e_{a,day}$ and $e_{a,Tn}$ for the development group of 20 stations.

An empirical model was developed using daily air temperature data, $l_{Ep,day}$, and $l_{P,ann}$ to predict $T_{d,day}$. The resulting regression equation is defined as

$$T_{d,est} = T_n\left[-0.127 + 1.121\,(1.003 - 1.444\,EF + 12.312\,EF^2 - 32.766\,EF^3) + 0.0006\,(T_x - T_n)\right] \quad (4)$$

where $T_{d,est}$ is the estimated mean daily dew point (K), T_n is the minimum daily air temperature (K), T_x

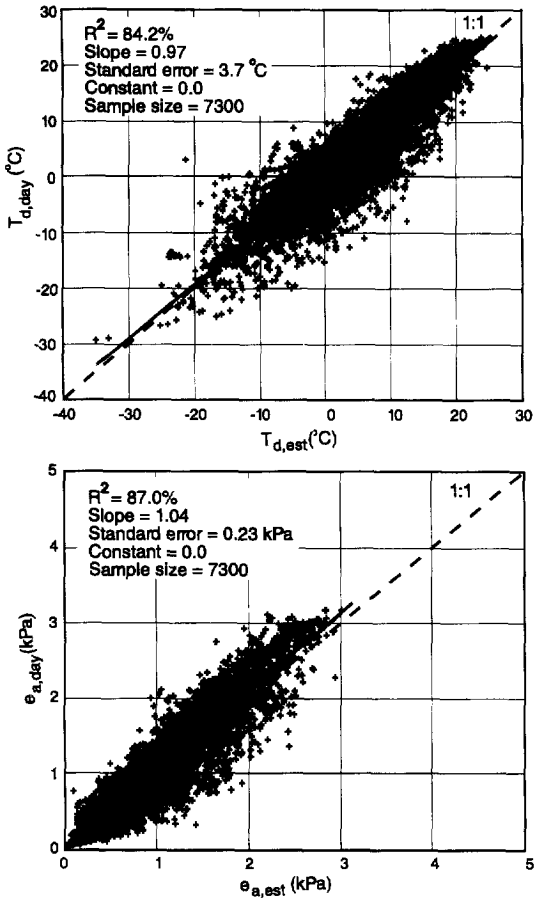

Fig. 3. Scatter plots showing linear regression results between $T_{d,day}$ and $T_{d,est}$, and $e_{a,day}$ and $e_{a,est}$ for the development group of 20 stations.

is the maximum daily air temperature (K), and $EF = l_{Ep,day}/l_{P,ann}$.

Application of Eq. (4) to the development group data resulted in a marked improvement in the relationship between T_n and humidity (Fig. 3). Both $T_{d,est}$ and the corresponding vapor pressure estimate ($e_{a,est}$) explained an improved 84% and 87% of the variation in daily humidities; application of the model also decreased standard errors of the regressions by 31% and 44% to approximately 3.7°C and 0.2 kPa, respectively. The model also had a marked effect on the slope of the relationship between estimated and measured vapor pressures, reducing the over-estimation of measured results from 21% to only 4%.

The test group data generally showed greater correlation between T_n and $T_{d,day}$ and corresponding humidities than the development group. T_n and $e_{a,Tn}$ explained 84% and 92% of the variance in $T_{d,day}$ and $e_{a,day}$ with standard regression errors of 4.5°C and 0.34 kPa, respectively. The slopes of the relationships were less than unity, however, indicating an approximate 17% and 15% over-estimation of $T_{d,day}$ and $e_{a,day}$, respectively. Application of Eq. (4) to the test group data explained an improved 91% and 97% of the variance in $T_{d,day}$ and $e_{a,day}$, reduced standard errors of the regressions by approximately 37%, and altered the slopes of the relationships from an approximate 16% over-estimation of measured humidity to only 4%.

The relationship between measured and estimated humidity differed between sites within different climate regions (Table 2). Mean daily vapor pressures derived from $T_{d,day}$ generally represented 41% and 65% of $e_{a,Tn}$ for arid and semi-arid sites, respectively. Vapor pressures derived from T_n also explained only 40% and 60% of the variation in $e_{a,day}$ in arid and semi-arid sites. Sites in other climate regions showed greater correspondence between

Table 2
Regression results for station data groups

Station group	Sample size	$e_{a,Tn}$ vs. $e_{a,day}$			$e_{a,est}$ vs. $e_{a,day}$			T_n vs. $T_{d,day}$			$T_{d,est}$ vs. $T_{d,day}$		
		R^2 (%)	Slope	SE (kPa)	R^2 (%)	Slope	SE (kPa)	R^2	Slope	SE (°C)	R^2	Slope	SE (°C)
Arid	1460	39.8	0.41	0.36	56.3	0.81	0.29	29.5	0.28	6.7	55.5	0.64	5.3
Semi-arid	5110	59.9	0.65	0.24	68.3	0.95	0.22	59.5	0.55	4.6	71.3	0.84	3.9
Marine-Coastal Med.	1460	75.8	0.95	0.18	82.3	1.05	0.15	76.7	0.93	2.3	80.4	1.06	2.1
Subpolar	1095	89.8	0.93	0.13	88.8	1.10	0.14	93.2	0.91	2.9	72.3	0.98	3.1
Humid continental	5475	91.9	0.96	0.19	91.5	1.09	0.19	93.0	0.94	2.9	92.8	1.05	2.9
Humid subtropical	4380	92.4	0.98	0.23	92.7	1.05	0.22	92.2	0.98	2.7	92.5	1.05	2.6

$e_{a,day}$ and $e_{a,Tn}$. T_n based vapor pressure estimates explained from 76% of the variance in $e_{a,day}$ at marine and coastal Mediterranean sites to approximately 91% of the variance in $e_{a,day}$ at subpolar, humid continental and humid subtropical locations; $e_{a,day}$ also represented greater than 93% of $e_{a,Tn}$ at these sites.

Model results were generally similar for sites with similar climate characteristics but showed marked differences between different climate regimes. Vapor pressures derived from T_n generally over-estimated $e_{a,day}$ by 59% and 35% at arid and semi-arid locations, respectively; application of Eq. (4) to these data reduced the over-estimation of $e_{a,day}$ to 19% and 5%. In other locations $e_{a,Tn}$ over-estimation of $e_{a,day}$ was generally small, ranging from 2% at humid subtropical sites to 7% at subpolar locations. Application of Eq. (4) to these data generally resulted in a slight under-estimation of $e_{a,day}$ from 5% at marine, coastal Mediterranean and humid subtropical sites to 10% at subpolar sites. Coefficients of determination and standard errors of the regression results at these sites generally remained consistent at approximately 88% and 0.2 kPa.

Results of the application of Eq. (4) to individual station data within the development and test station groups are summarized in Tables 3 and 4, respectively. The magnitude of the reduction in error was greatest for stations in arid climate regimes which showed the largest differences between $e_{a,Tn}$ and $e_{a,day}$. Standard errors of the vapor pressure estimates at these sites were reduced from 0.7 to 1.0 kPa, resulting in an average error of approximately 0.3 kPa. These results constituted error reductions from 64 to 80% over unadjusted results. Phoenix, AZ and China Lake, CA, for example, showed respective standard estimation errors of 1.44 and 1.00 kPa with summer estimation error maxima near 3.4 kPa for unadjusted results. Application of Eq. (4) to the data reduced respective standard errors of the estimates by 69% and 80% to approximately 0.3 kPa.

Model results were also favorable for stations in semi-arid locations. Model adjustment of the data were minimal during the winter months when estimation errors were small. The model was quite effective, however, in reducing large estimation errors which were more prevalent during the summer months. Standard errors of the estimate for unadjusted results at Boise, ID and Salt Lake City, UT, for example, ranged from approximately 0.1 kPa

Table 3
Impact of regression (Eq. (4)) on development group humidity estimates

Development group	$l_{P,ann}/l_{Ep,ann}$	SEE T_n (°C)	SEE $T_{d,est}$ (°C)	Δ SEE (°C)	SEE $e_{a,Tn}$ (kPa)	SEE $e_{a,est}$ (kPa)	ΔSEE (kPa)
China Lake, CA	0.02	13.5	6.6	−7	1.00	0.22	−0.8
Las Vegas, NV	0.06	14.9	5.5	−9	1.28	0.29	−1.0
Reno, NV	0.08	7.7	3.4	−4	0.50	0.13	−0.4
Tucson, AZ	0.14	11.6	6.8	−5	1.09	0.38	−0.7
Salt Lake City, UT	0.24	6.5	3.5	−3	0.59	0.22	−0.4
Spokane, WA	0.29	4.9	3.1	−2	0.36	0.16	−0.2
Abiline, TX	0.37	5.2	4.3	< −1	0.50	0.27	−0.2
San Diego, CA	0.37	2.9	2.7	< −1	0.26	0.23	< −0.1
Pierre, SD	0.38	3.1	3.3	< 1	0.21	0.24	< 0.1
Topeka, KS	0.48	2.5	3.0	< 1	0.19	0.27	< 0.1
Springfield, IL	0.48	2.9	3.1	< 1	0.22	0.29	< 0.1
Cleveland, OH	0.56	2.8	2.5	< −1	0.22	0.20	< −0.1
Madison, WI	0.65	2.4	2.5	< 1	0.15	0.18	< 0.1
Richmond, VA	0.65	3.0	3.0	< 1	0.22	0.26	< 0.1
Charleston, SC	0.79	2.6	2.7	< 1	0.19	0.26	< 0.1
Seattle, WA	0.80	2.2	1.8	< −1	0.17	0.12	< −0.1
Eugene, OR	0.87	2.3	2.2	< −1	0.16	0.15	< −0.1
Boston, MA	0.88	4.3	3.9	< −1	0.32	0.26	< −0.1
New Orleans, LA	1.13	2.6	2.5	< −1	0.31	0.26	< −0.1
Juneau, AK	2.39	2.7	2.6	< −1	0.11	0.10	< −0.1

Table 4
Impact of regression (Eq. (4)) on test group humidity estimates

Test group	$l_{P,ann}/l_{Ep,ann}$	SEE T_n (°C)	SEE $T_{d,est}$ (°C)	Δ SEE (°C)	SEE $e_{a,Tn}$ (kPa)	SEE $e_{a,est}$ (kPa)	Δ SEE (kPa)
Bishop, CA	0.09	7.0	4.7	−2	0.40	0.20	−0.2
Phoenix, AZ	0.11	12.7	5.9	−7	1.44	0.42	−1.0
Grand Junction, CO	0.13	9.2	4.3	−5	0.67	0.23	−0.4
Winnemucca, NV	0.13	5.8	4.3	−2	0.32	0.17	−0.2
Fresno, CA	0.15	4.7	3.1	−2	0.47	0.21	−0.3
Albuquerque, NM	0.16	9.8	5.5	−4	0.74	0.29	−0.4
Boise, ID	0.17	5.5	3.6	−2	0.42	0.19	−0.2
Pendleton, OR	0.23	5.7	3.1	−3	0.44	0.19	−0.3
Casper, WY	0.23	5.9	4.2	−2	0.36	0.21	−0.2
Billings, MT	0.25	5.9	4.1	−2	0.40	0.21	−0.2
Denver, CO	0.27	5.9	4.8	−1	0.37	0.23	−0.1
Fairbanks, AK	0.33	3.6	3.6	<1	0.18	0.19	<0.1
Fargo, ND	0.40	3.3	3.3	0	0.19	0.21	<0.1
Lincoln, NE	0.40	2.9	3.2	<1	0.18	0.26	<0.1
Anchorage, AK	0.51	3.0	3.2	<1	0.14	0.16	<0.1
Knoxville, TN	0.52	2.5	2.6	<1	0.17	0.22	<0.1
Augusta, GA	0.56	2.6	2.9	<1	0.19	0.25	<0.1
Asheville, NC	0.59	2.5	2.9	<1	0.15	0.23	<0.1
Louisville, KY	0.60	3.5	3.1	<−1	0.31	0.24	<−0.1
South Bend, IN	0.65	2.7	2.8	<1	0.18	0.22	<0.1
Diluth, MN	0.70	3.2	3.2	<1	0.16	0.20	<0.1
Concord, NH	0.74	3.1	3.1	<1	0.18	0.20	<0.1
Little Rock, AR	0.75	3.0	3.1	<1	0.22	0.28	<0.1
Tulsa, OK	0.76	2.6	2.6	0	0.23	0.23	0.0
Huntsville, AL	0.77	2.2	2.4	<1	0.17	0.21	<0.1
Detroit, MI	0.77	2.4	2.3	<−1	0.16	0.17	<0.1
Harrisburg, PA	0.80	2.9	2.9	<1	0.18	0.19	<0.1
Miami, FL	0.84	2.5	2.0	<−1	0.37	0.27	−0.1
Jackson, MS	0.86	2.2	2.3	<1	0.19	0.24	<0.1
Portland, ME	0.93	2.8	2.8	<1	0.16	0.17	<0.1
Des Moines, IA	1.13	2.1	2.2	<1	0.13	0.17	<0.1
Astoria, OR	1.97	2.3	2.2	<−1	0.15	0.15	<−0.1

during the winter months to 0.8 kPa during the summer. The model reduced the average error by only 0.01 kPa (14%) during the winter but reduced the average error during the summer months by 0.5 kPa (71%) and 0.7 kPa (67%), respectively. On an annual basis, standard errors of the estimate were reduced from 0.1 to 0.4 kPa to approximately 0.2 kPa at semi-arid sites, which represented reductions from 27 to 80% over unadjusted results.

The model had minimal effect on data from other climate regimes. Standard errors between T_n and $T_{d,day}$ at these sites were generally less than 4°C which corresponded to standard vapor pressure estimation errors of less than 0.4 kPa. Model adjustment of these data resulted in changes in $T_{d,day}$ estimation errors between ±1°C and corresponding changes in $e_{a,day}$ estimation errors between ±0.1 kPa.

The ratio of $l_{P,ann}$ to $l_{Ep,ann}$ provided a useful mechanism for distinguishing sites, where errors between $T_{d,day}$ and T_n based vapor pressures were large, from sites where errors between $e_{a,day}$ and $e_{a,Tn}$ were relatively small. Stations where $l_{P,ann}$ represented less than approximately 30% of $l_{Ep,ann}$ generally represented arid and semi-arid sites where Eq. (4) yielded improved results over unadjusted T_n based humidity estimates. The model generally had minimal effect at sites where $l_{P,ann}$ constituted greater proportions of $l_{Ep,ann}$; differences between $e_{a,day}$ and $e_{a,Tn}$ at these sites also tended to be much smaller than at arid and semi-arid locations.

6. Summary and conclusions

The objectives of this investigation were to assess the relationships between $T_{d,day}$ and T_n for different climate regimes in order to develop a method for improving T_n based humidity estimates using daily weather station data. Three general trends were observed in the data. Sites with arid climate characteristics tended to show large daily differences between T_n and $T_{d,day}$ over the entire year, corresponding to average daily differences between $e_{a,day}$ and $e_{a,Tn}$ from 0.8 to 1.2 kPa. Sites with semi-arid climate characteristics showed a large degree of seasonality in the results, where daily differences between $T_{d,day}$ and T_n were minimal from October to April but increased markedly from May to September in response to warmer, drier conditions. These results corresponded to average daily differences between $e_{a,day}$ and $e_{a,Tn}$ from 0.1 to 0.6 kPa between winter and summer months, respectively. Sites in other climate regimes generally showed small differences between T_n and $T_{d,day}$ over the entire year, corresponding to average daily differences of less than 0.3 kPa between $e_{a,day}$ and $e_{a,Tn}$.

An empirical model was developed to improve the accuracy of T_n based humidity estimates using daily air temperature, annual precipitation and estimated daily potential evapotranspiration. Model results were favorable at arid sites, reducing standard errors of estimated vapor pressures from 0.7 to 1.0 kPa. These results constituted error reductions from 64 to 80% over unadjusted results. The model was also effective at semi-arid sites, reducing vapor pressure estimation errors from 0.1 to 0.4 kPa, which represented error reductions from 27 to 80% over unadjusted results. The model had minimal effect in other climate regimes where standard errors of T_n based vapor pressure estimates were less than 0.4 kPa. Model adjustment of these data resulted in changes in vapor pressure estimation errors between ± 0.1 kPa.

The ratio of annual precipitation to estimated annual evapotranspiration provided an effective means for distinguishing sites where T_n based humidity estimates were fairly accurate from sites where estimation errors were large. Annual precipitation represented greater than 30% of $l_{Ep,ann}$ at sites with marine, coastal Mediterranean, humid continental, subpolar and humid subtropical climate characteristics; daily differences between $e_{a,day}$ and $e_{a,Tn}$ were relatively small at these sites over the entire year. Sites where $l_{P,ann}$ was less than approximately 30% of $l_{Ep,ann}$ generally represented arid and semi-arid locations where T_n based humidity estimation errors were large and model results were favorable. Overall, the results of this investigation provide a simple method for identifying sites where T_n based humidity estimates are generally accurate and extend the usefulness of these estimates over a greater range of conditions using additional information provided by general weather station data.

Acknowledgements

This research was funded under NASA grants NAGW-4511, NAGS-2297, and NAGW-4234. Data were provided by the US Department of Commerce, National Oceanic and Atmospheric Administration, National Environmental Satellite Data and Information Service, National Climatic Data Center, Asheville, NC.

References

Bristow, K.L. and Campbell, G.S., 1984. On the relationship between incoming solar radiation and daily maximum and minimum temperature. Agric. For. Meteorol., 31: 159–166.

Brutsaert, W., 1982. Evaporation into the Atmosphere. Reidel, Dordrecht, 299 pp.

Campbell, G.S., 1977. An Introduction to Environmental Biophysics. Springer, New York, 159 pp.

Choudhury, B.J. and Monteith, J.L., 1986. Implications of stomatal response to saturation deficit for the heat balance of vegetation. Agric. For. Meteorol., 36: 215–225.

Finklin, A.I., 1983. Summarizing weather and climatic data—A guide for wildland managers. USDA Technical Report INT-148, 43 pp.

Friend, A.D., 1996. Parameterization of a global daily weather generator for terrestrial ecosystem and biogeochemical modelling. Ecol. Modelling (submitted).

Glassy, J.M. and Running, S.W., 1994. Validating diurnal climatology logic of the MT-CLIM model across a climatic gradient in Oregon. Ecol. Appl., 4(2): 248–257.

Grantz, D.A., 1990. Plant response to atmospheric humidity. Plant, Cell Environ., 13: 667–679.

Hansen, J., Lacis, A., Rind, D., Russell, G., Stone, P., Fung, I., Ruedy, R. and Lerner, J., 1984. Climate sensitivity: analysis of feedback mechanisms. In: J.E. Hansen and T. Takahashi (Edi-

tors), Climate Processes and Climate Sensitivity. Geophysical Monographs, AGU, Washington, DC, 29, pp. 130–163.

Hogg, R.V. and Ledolter, J., 1987. Engineering Statistics. Macmillan, New York, 419 pp.

Hungerford, R.D., Nemani, R.R., Running, S.W. and Coughlan, J.C., 1989. MTCLIM: a mountain microclimate simulation model. Res. Pap. INT-414, USDA Forest Service, 52 pp.

James, W.E., 1953. Forecasting ground frost. Meteorol. Mag., 82(969): 91

Kaufmann, M.R., 1984. Effects of weather and physiographic conditions on temperature and humidity in subalpine watersheds of the Fraser Experimental Forest. Res. Pap. RM-251, USDA Forest Service, 9 pp.

Kittel, T.G.F., Rosenbloom, N.A., Painter, T.H. and Schimel, D.S., 1996. The VEMAP integrated database for modeling United States ecosystem/vegetation sensitivity to climate change. J. Biogeogr., in press.

Köppen, W., 1931. The Climates of the Earth. DeGruyter, Berlin, 388 pp. (In German.)

Korner, C. and Bannister, Up., 1985. Stomatal responses to humidity in *Nothofagus menziesii*. N.Z. J. Bot., 23: 425–429.

Marks, D., Dozier, J. and Davis, R.E., 1992. Climate and energy exchange at the snow surface in the alpine region of the Sierra Nevada, 1. Meteorological measurements and monitoring. Water Resourc. Res., 28 (11): 3029.

McCutchan, M.H., 1977. Climatic features as a fire determinant. Gen. Tech. Rep. W-3, USDA Forest Service, 11 pp.

Monteith, J.L. and Unsworth, M.H., 1990. Principles of Environmental Physics, 2nd edn. Edward Arnold, New York, 291 pp.

National Weather Service, 1988. Surface Observations, Federal Meteorological Handbook No. 1 (FCM-H1-1988). Office of the Federal Coordinator, Department of Commerce, Washington, DC.

Priestley, C.H.B. and Taylor, R.J., 1972. On the assessment of surface heat flux and evaporation using large-scale parameters. Mon. Weather Rev., 100(2): 81–92.

Running, S.W. and Coughlan, J.C., 1988. A general model of forest ecosystem processes for regional applications. I. Hydrologic balance, canopy gas exchange and primary production processes. Ecol. Modelling, 41: 125–154.

Running, S.W., Nemani, R.R. and Hungerford, R.D., 1987. Extrapolation of synoptic meteorological data in mountainous terrain, and its use for simulating forest evapotranspiration. Can. J. For. Res., 17: 472–483.

Thornthwaite, C.W., 1948. An approach toward a rational classification of climate. Geogr. Rev., 38: 55–94.

Weast, R.C. (Editor), 1983. CRC Handbook of Chemistry and Physics. CRC Press, Boca Raton, FL, 64, pp. 192–194.